**INCREASING DIVERSITY OF ORDINARY CHONDRITE AND RUMURUTI-TYPE CHONDRITE CLASTS IN POLYMICT UREILITES.** C.A. Goodrich,[1] A.H. Treiman,[1] N.T. Kita,[2] and C. Defouilloy.[2] [1]Lunar and Planetary Institute, 3600 Bay Area Blvd., Houston, TX 77058 USA. goodrich@lpi.usra.edu. [2]WISC-SIMS University of Wisconsin, Madison, WI 53706 USA.

**Introduction:** Polymict ureilites are fragmental breccias interpreted to represent regolith formed on a ureilitic body [1,2]. They consist of ≥95% clasts of various ureilite types (olivine-pyroxene rocks of Fo 75-95), a few % indigenous feldspathic clasts [3-5], and a few % foreign clasts. The latter provide information on the chemical/isotopic diversity of materials in the regions(s) in which ureilitic regolith formed [1,2,6]. Previous work has identified a variety of foreign clasts. However, most of these have not been studied in detail, and their full diversity is not known. We have been searching for foreign clasts in polymict ureilites [7-9] by targeting clasts that are: 1) feldspathic (ureilites contain no feldspar); 2) FeO-rich (ureilites are Mg-rich); and/or 3) olivine-rich (indigenous feldspathic clasts are pyroxene-rich). We describe 12 new chondritic clasts and discuss implications.

**Methods:** We studied 11 sections of 7 polymict ureilites by SEM and EMPA at ARES, JSC and Dept. Geol., U. Mass. Oxygen isotopes were analyzed by SIMS at Wisc-SIMS following [10] with a 3 μm spot.

**Isolated Chondrules:** Three clasts have "droplet" shapes and textures consistent with being chondrules. Dar al Gani (DaG) 319_005 clast 5 (~0.5 mm) can be classified as PO (Fig. 1a). It contains olivine phenocrysts (Fo ~92-89), smaller olivines (Fo 83-68), and feldspathic matrix with skeletal olivine. FeO-MnO contents of olivine (Fig. 2) are consistent with type 3.1-3.5 OC or 3.1-3.2 RC. CaO suggests 3.1-3.2.

Elephant Moraine (EET) 83309,16 clast 1 (~0.5 mm) can be classified as POP. It consists of eu/subhedral olivine and opx in glassy (?) feldspathic mesostasis. Olivine grains are Fo ~90-78. Opx is Wo ~1-3, mg# 92-93, with olivine (Fo 86) inclusions and rims. FeO-MnO contents of olivine are consistent with type 3.0-3.7 OC or 3.1-3.2 RC (Fig. 2). CaO suggests 3.0-3.4 OC or 3.1-3.2 RC.

DaG 319_003 clast 23 (~0.2 mm) can be classified as PO. It consists of subhedral olivine and minor opx, with feldspathic mesostasis. Olivine is Fo 80-81. Opx is Wo ~1, mg# 83. FeO-MnO contents indicate type 3.1-6 OC or 3.8-6 RC (Fig. 2). CaO suggests type 4-6. The chondrule is intact, so it is probably type 4.

**OC Clasts:** DaG 999 clast 1 (~800 μm) contains two partial PP chondrules (Fig. 1b), which consist of opx phenocrysts and feldspathic mesostasis with mafic crystallites. The opx is Wo ~0.5, mg# 78-81 and shows "patchy" zoning of mg# similar to that in type 3.8 RC and 3.6-3.9 OC [11,12]. The rest of the clast consists of equigranular olivine, with minor intergranular pyroxenes, feldspathic mesostasis, chromite and troilite. Olivine is Fo 71-73; pyroxenes are Wo 0.3, mg# 76 and Wo 60, mg# 78; mesostasis has ~10% $Na_2O$ and 1-2% $K_2O$; chromites are Cr# 0.9, fe# ~0.8, with ~3% $TiO_2$. FeO-MnO (Fig. 2) and CaO of olivine are consistent with type 3.7-6 LL. Based on patchy zoning in pyroxene [12], it is LL 3.7-3.9.

**Incompletely Equilibrated R-Chondrite Clasts:** Frontier Mountain (FRO) 90200 clast 26 (~425×130 μm) consists largely of fine-grained (tens of nm-sized) olivine of Fo 52-56, with rare grains (10-20 μm) of Mg-rich olivine (Fo 94) and opx (mg# 97) (Fig. 1c). Minor phases are chromite and Fe,Ni metal (34% Ni). Other areas show coarse euhedral olivine (~2-15 μm) in glassy (?) feldspathic matrix (Fig. 1c, bottom left). Coarse olivine is Fo 60-62; pyroxenes are Wo ~2, mg# 78 and Wo ~36, mg# 77. FeO-MnO (Fig. 2) and CaO of olivine are consistent with type 3.8-6 RC. The preservation of Mg-rich olivine and pyroxene in FeO-rich matrix suggests type 3.8 [11,13,14].

Oxygen isotope compositions of select olivine and pyroxene in clast 26 were obtained by SIMS. Results (Fig. 3) show $\Delta^{17}O$ from +4.6‰ to -6.0‰ and a trend distinct from that of ureilites. One datum (Fo 59) plots above the terrestrial fractionation line (TF), similar to altered FeO-rich olivine in an R3 [17]. However, the rest (both Mg-rich and Fe-rich) plot below TF, similar to CC and unlike most olivine in RC [15,16].

FRO 03022 clast 1 (~1.3 mm) consists mostly of equigranular olivine (Fo 66-67), with intergranular augite (Wo ~38, mg# 70-73) and Si-rich mesostasis (Fig. 1d). It also contains patchily-zoned opx (Wo <1, mg# ~73 & 96). Several areas may be relict chondrules (Fig. 1d). One ~200 μm-sized area of olivine is concentrically zoned from Fo 80–66 (Fig. 1c). FeS is abundant. Fe,Ni metal occurs with inclusions of Ca-phosphate. FeO-MnO (Fig. 2) and CaO of olivine are similar to but extend the ranges for type 3.8-6 RC. Patchy opx suggests type 3.8 [11,12].

**Equilibrated RC Clasts:** Five clasts have mineralogy (mainly olivine), textures (equigranular), and mineral compositions (e.g., Fo 60-64; Fig. 2) consistent with equilibrated RC. However, they differ in abundances and compositions of pyroxenes, plagioclase, phosphate, spinels (e.g., magnetite vs. chromite) and sulfides (pentlandite vs. troilite).

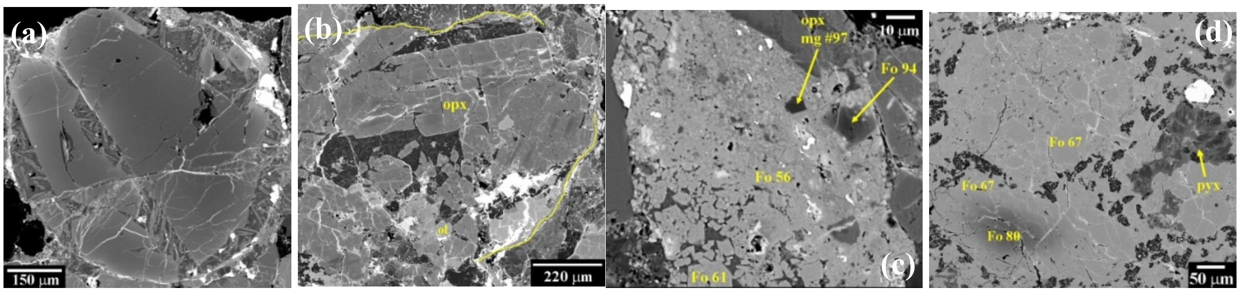


**Fig. 1.** (a) DaG 319_005 clast 5, PO chondrule, type 3.1-3.2. (b) DaG 999 clast 1 (LL3.7-3.9). Partial PP chondrule. (c) FRO 90200 clast 26 (R3.8). Fine-grained (nm scale) matrix of Fo 52-56 olivine with relict Mg-rich olivine (Fo 94) and pyx. Other areas (lower left) show euhedral olivine (Fo ~62) in glass (?). (d) FRO 03022 clast 1 (R3.8). Area of equigranular olivine (Fo 67) with intergranular augite, and area of zoned olivine Fo 80–67. Si-rich mesostasis and patchily-zoned pyx around olivine areas.

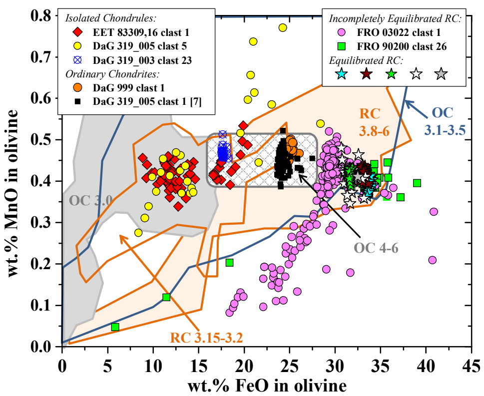


**Fig. 2 (left).** FeO vs. MnO in olivine in studied clasts, compared with various petrologic types of OC & RC.

**Fig. 3 (right).** Oxygen-isotopes of FRO 90200 clast 26 from SIMS, compared with bulk ureilites, OC, RC and olivine from RC.

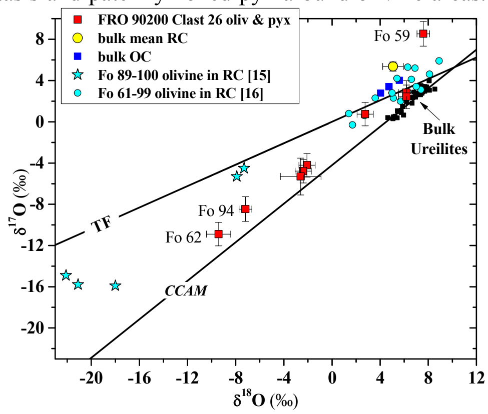


**Discussion:** Polymict ureilites are exceptional for the diversity of their foreign clasts, covering all major chondrite classes, as well as achondrites [1,2,18]. Our results and [7,19] show that these clasts are also diverse within each class/group, and within small volumes of ureilitic regolith (portions of thin sections).

This diversity indicates that either 1) ureilitic regolith was particularly efficient at preserving fragments of impactors; 2) ureilitic regolith was exposed to a particularly large range of environments (heliocentric distances) due to orbital migration [6]; or 3) most impactors into ureilitic regolith were complex breccias. The last seems least likely.

The 3 isolated chondrules must derive from at least 2 different chondrites (based on petrologic types), but it is unlikely that their hosts were any of the chondritic clasts observed. We may not be able to determine whether they derive from OC or RC, since chondrules in OC and RC apparently formed from a common chemical and oxygen isotope reservoir [13,16,20,21].

The incompletely equilibrated RC clasts extend the diversity of RC materials [20,22]. FRO 90200 clast 26 (R3.8) may have been partially impact melted (coarse, euhedral olivine areas; cf. [20]). The oxygen isotope data suggest possible impact mixing with CC material. Sharp boundaries of the clast with its host indicate that this occurred before incorporation into ureilitic regolith. Although most of FRO 03022 clast 1 is similar to equilibrated RC, its dominant olivine composition (Fo 67) is more Mg-rich than in equilibrated RC, and the olivine FeO-MnO trend does not parallel that of known RC (Fig. 2). The RC clasts show differences in type of spinel and sulfide/metal assemblage that may reflect a range of oxidation states, extending an OC→RC trend. Polymict ureilites may sample a different population of RC material than individual meteorites arriving at Earth. We will conduct additional petrologic and oxygen isotope studies on these clasts to constrain their origin.

**References:** [1] Goodrich C.A. et al. (2004) Chemie der Erde 64, 283. [2] Downes H. et al. (2008) GCA 72, 4825. [3] Ikeda Y. et al. (2000) Ant. Met. Res. 13, 177. [4] Cohen B.A. et al. GCA 68, 4249. [5] Kita N.T. et al. (2004) GCA 68, 4213. [6] Goodrich C.A. et al. (2015) MAPS 50, 782. [7] Goodrich C.A. et al. (2015) LPSC 46, #1214. [8] Goodrich C.A. et al. (2015) 78th MSM, #5048. [9] Goodrich C.A. et al. (2015) 78th MSM, #5048. [10] Ushikubo T. et al. (2012) GCA 90, 242. [11] Weisberg M.K. et al. (1991) GCA 55, 2657. [12] Tsuchiyama A. et al. (1988) NIPR Symp. Ant. Met. 1, 173. [13] Bischoff A. (2000) MAPS 45, 699. [14] Jäckel A. et al. (1996) LPSC 27, 595. [15] Pack A. et al. (2004) GCA 68, 1135. [16] Greenwood J.P. et al. (2000) GCA 64, 3897. [17] Kita N.T. et al. (2013) LPSC 44, #1784. [18] Bischoff A. et al. (2004) in MESS II, 679. [19] Horstmann M. & Bischoff A. (2014) Chemie der Erde 74, 149. [20] Bischoff A. et al. (2011) Chemie der Erde 71, 101. [21] Kita N.T. et al. (2015) 46th LPSC, #2053. [22] Horstmann M. et al. (2010) MAPS 45, 1638.